

# Nonlinear ac responses of erythrocyte suspensions: Experiment and theory

J. T. Zhu,<sup>a)</sup> W. J. Tian,<sup>b)</sup> S. Zheng,<sup>c)</sup> J. P. Huang,<sup>d)</sup> and L. W. Zhou<sup>e)</sup>

*Surface Physics Laboratory (National Key Laboratory) and Department of Physics, Fudan University, Shanghai 200433, China*

(Received 26 July 2007; accepted 26 September 2007; published online 11 December 2007)

When a suspension consisting of electric particles having nonlinear characteristics is subjected to a sinusoidal alternating current (ac) electric field, the electric response will generally consist of ac fields at frequencies of higher-order harmonics. We experimentally report on harmonic generation by erythrocytes subjected to an ac electric field. We find that both even and odd harmonics are sensitive to cell shapes, conductivities, field frequencies, and field magnitude. Theoretical analysis based on a phenomenological model yield predictions that are in excellent agreement with the experiments. Thus, it becomes possible to detect nonlinear characteristics, shapes, and conductivities of erythrocytes by measuring such ac responses. © 2007 American Institute of Physics. [DOI: 10.1063/1.2817398]

## I. INTRODUCTION

Erythrocytes have been extensively studied, ranging from dynamic and dielectric behaviors<sup>1–3</sup> to biological activities,<sup>4</sup> and from clustering characteristics<sup>5</sup> to softness.<sup>6–8</sup> Erythrocytes are the most common type of blood cell and the vertebrate body's principal means of delivering oxygen from the lungs or gills to body tissues via the blood. As a result of the lack of nucleus and organelles, most mammalian erythrocytes cannot produce new structural or repair proteins or enzymes and their lifespan is limited. In general, each erythrocyte has a lifespan of about 4 months.

When a suspension consisting of electric particles having nonlinear characteristics is subjected to a sinusoidal alternating current (ac) electric field, the electric response will, in general, consist of ac fields at frequencies of the higher-order harmonics (for example, see Refs. 9–11). We shall report on harmonic generation by erythrocytes subjected to an ac electric field. It is known that an external ac electric field can polarize living erythrocytes in suspensions, which causes enormous electric or dielectric responses,<sup>12</sup> and modulates the membrane potential of each cell. In general, a field of low magnitude can modulate the normal membrane potential, creating an amplified net field modulation across a plasma membrane of a cell. Membrane proteins are candidates for nonlinear responses<sup>13</sup> as they cannot rotate within the membrane and dissipate energy through Debye-like relaxation, and also as any transmembrane domains with dipole moments interact with the greatly amplified ac field. The modulated oscillatory transmembrane potential drives membrane proteins to change their conformational states.<sup>14</sup> Such change alters the energy landscape seen by the ions.<sup>15</sup> Once the ions become trapped in a well, a conformational

change facilitated by an external field takes place. The modulated transmembrane potential affects the potential barrier seen by the ion, thus increasing or decreasing the probability for the ion to hop into the adjacent well.<sup>16</sup> In other words, such time-dependent conformational changes can induce pumps to transport ions,<sup>15,17–19</sup> which creates a nonlinear response reflected by the harmonic generation.<sup>16,20,21</sup> It is well known that even harmonic generation appears in various materials lacking inversion symmetry, e.g., erythrocyte membranes made of proteins embedded in a lipid bilayer that just breaks inversion symmetry. On the other hand, odd harmonic generation comes to appear in materials either lacking or having inversion symmetry. For more details on the origin of harmonic generation, please refer to Sec. V.

This article is organized as follows. In Sec. II, our experiment is conducted to investigate the harmonic generation of erythrocytes. In Sec. III, we put forth a theory based on a phenomenological model, in order to account for the experimental results, which is followed by Sec. IV in which our results are presented. Some discussion can also be found in Sec. IV. The paper ends with a conclusion in Sec. V.

## II. EXPERIMENT

We experimentally investigate harmonic generation by erythrocytes in response to an electric field with low magnitudes and low frequencies. The detailed illustration of the setup of experiment is displayed in Fig. 1, where  $r=50\ \Omega$  denotes the inner resistance of the ac power, and  $R=10\ \Omega$  is the resistance to prevent power from being overloaded during the experiments. Both second and third harmonics of currents can be measured from the outputs,  $S_+$  and  $S_-$ .

The porcine blood was used in the experiment. To proceed, the erythrocytes must be separated from blood plasma by centrifuge. During the experiment we adjusted the rotate speed to 1500 circle/min. Besides the erythrocytes, the blood also contains leukocytes, inorganic salt, etc. However, these

<sup>a)</sup>Electronic mail: 031019032@fudan.edu.cn.

<sup>b)</sup>Electronic mail: 062019019@fudan.edu.cn.

<sup>c)</sup>Electronic mail: 031019012@fudan.edu.cn.

<sup>d)</sup>Corresponding author. Electronic mail: jphuang@fudan.edu.cn.

<sup>e)</sup>Corresponding author. Electronic mail: lwzhou@fudan.edu.cn.

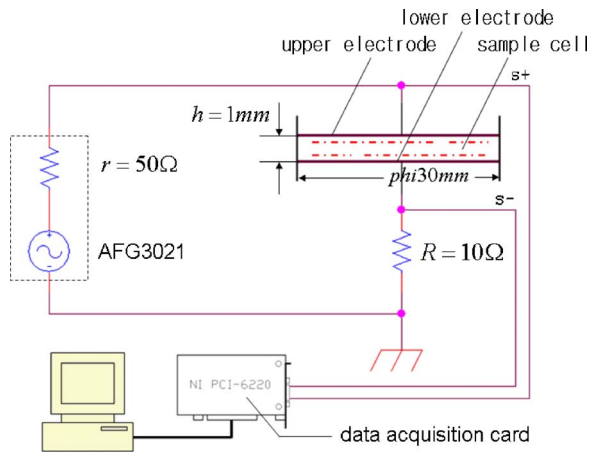


FIG. 1. (Color online) Sketch of the experimental setup.  $r=50\ \Omega$  denotes the inner resistance of the ac power, and  $R=10\ \Omega$  the resistance to prevent power from overload during the experiment. The harmonic currents can be measured from the outputs,  $S+$  and  $S-$ .

ingredients can bring disturbing effects to the experiment. For focusing on erythrocytes only, the following steps were taken to purify erythrocytes:

Step 1. Put 6 ml blood in a centrifugal tube of 20 ml and rotate it for about 5 min. Then the blood will be divided into two layers.

Step 2. Take away the buffy coat and keep adding 10% sucrose solution to the tube till the total volume reaches at least to 18 ml and then rotate it for another 5 min.

Repeat Step 2 for 5 times and take away the buffy coat again and again. Eventually we obtained ideal samples needed. It is difficult to measure the volume fraction of erythrocytes directly in this experiment, here we used the following method. First, the sample was diluted with 10% sucrose solution (which showed to have no harmonic currents within the range of the voltage and frequency of our interest) to achieve 0.1% volume fraction. Then a hemacytometer was used to counter the number of erythrocytes, and we found that the number density is  $4.8625 \times 10^9\ \text{ml}^{-1}$ . By

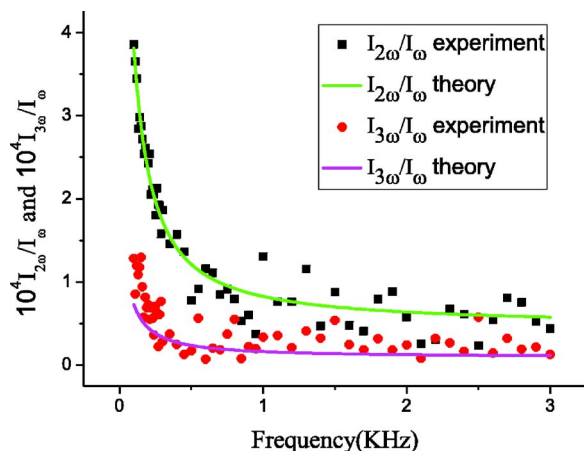


FIG. 2. (Color online) Fitting (lines) of the experimental data (symbols) of second and third harmonics to basic harmonics,  $I_{2\omega}/I_\omega$  and  $I_{3\omega}/I_\omega$ , for  $\tilde{U}=5.0\ \text{V}$ . Parameters used for theoretical fitting (lines):  $d=1\ \text{mm}$  (obtained from experiment),  $p=73\%$  (obtained from experiment),  $g_\perp=0.29$  (obtained from experiment),  $\xi_1=5.0 \times 10^{-7}\ \text{S/V}$ ,  $\chi_1=4.0 \times 10^{-11}\ \text{Sm/V}^2$ ,  $\sigma_{1H}=0.8\ \text{S/m}$ ,  $\delta\sigma=-0.66\ \text{S/m}$ ,  $\sigma_2=0.03\ \text{S/m}$ , and  $\omega_0=3.0 \times 10^3\ \text{rad/s}$ .

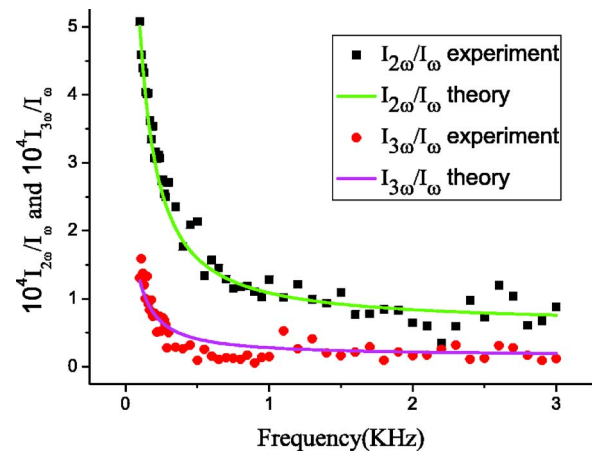


FIG. 3. (Color online) Same as Fig. 2, but for  $\tilde{U}=6.6\ \text{V}$ .

seeing one model erythrocyte as an oblate spheroid, the volume of the erythrocyte in use is about  $1.5 \times 10^{-10}\ \text{ml}$ , and the depolarization factor  $g_\perp$  perpendicular to the symmetrical axis is about 0.29. Thus, we obtained the volume fraction  $p$  of erythrocytes in our sample about 73%. The power we used is an arbitrary/function generator made by Tektronix with the model AFG3021. By using the data acquisition card NI PCI-6220 we acquired a group of voltage data between the outputs,  $S+$  and  $S-$ , when the frequency was shifted from 100 Hz to 3 kHz at three different voltages, which correspond to net voltages for the sample, 5.0, 6.6, and 8.3 V, respectively. For every frequency interval of 10 or 50 Hz we recorded 10 000 points, from which we got the values for voltages at basic, second and third harmonics. Cares were taken in three aspects when the experiment was conducted: The electrodes of the sample cell should not be made by alloy, to avoid the battery effect, heparin sodium should be added to prevent the blood from curdling, and the erythrocytes must not be mixed with too much blood plasma and inorganic salt because the latter can bring some unexpected background noises.

The experimental data of second and third harmonics of currents of the erythrocyte suspensions are displayed in Figs. 2–4, which clearly show that erythrocytes have nonlinear responses to electric fields. It is shown that the current harmonics increase for either decreasing field frequency or in-

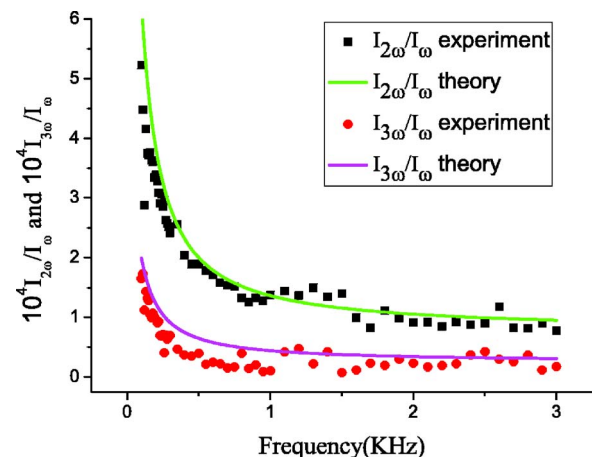


FIG. 4. (Color online) Same as Fig. 2, but for  $\tilde{U}=8.3\ \text{V}$ .

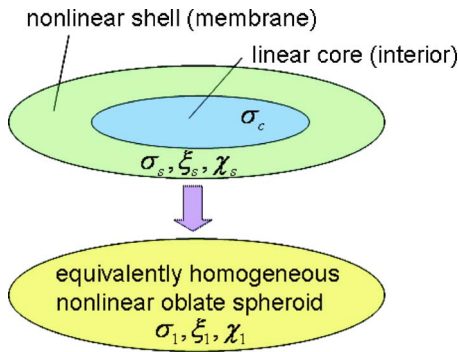


FIG. 5. (Color online) Sketch of the equivalence between an erythrocyte (upper panel) and a homogeneous oblate spheroid (lower panel).

creasing applied voltage of the electromotive force (emf). In addition, we have also investigated harmonic generation for different concentrations of the erythrocytes, and obtained the results similar to those reported in Figs. 2–4. We find that higher concentration yields stronger responses of harmonics.

### III. THEORY

#### A. Equivalent nonlinear characteristic of an erythrocyte

Now we are in a position to establish a phenomenological model to interpret the experimental results displayed in Figs. 2–4. In general, many mammalian erythrocytes are biconcave disks, flattened and depressed in the center, with a dumb-bell shaped cross section. In what follows, for simplification, we model the geometrical shape of erythrocytes as an oblate spheroid with two depolarization factors,  $g_{\parallel}$  and  $g_{\perp}$ . They satisfy the sum rule  $g_{\parallel} + 2g_{\perp} = 1$ , with  $1/3 < g_{\parallel} < 1$ .<sup>22,23</sup> The oblate spheroid is composed of a core (namely, interior or hemoglobin of the erythrocyte) and a shell (i.e., biological membrane of the erythrocyte). As ion translocation can yield nonlinear characteristics of biological cells, we are allowed to set the shell to be nonlinear, whereas the core is linear. The (linear) conductivities of the shell and core are denoted as  $\sigma_s$  and  $\sigma_c$ , respectively. And the second- and third-order nonlinear susceptibilities of the shell are, respectively, represented as  $\xi_s$  and  $\chi_s$ . That is, there is a constitutive relation between the current density  $J_s$  and electric field  $E_s$  in the shell,

$$J_s = (\sigma_s + \xi_s E_s + \chi_s E_s^2) E_s \equiv \tilde{\sigma}_s E_s. \quad (1)$$

An alternative constitutive relation between the current density  $J_c$  and electric field  $E_c$  in the core is

$$J_c = \sigma_c E_c. \quad (2)$$

For convenience, the core-shell oblate spheroid (erythrocyte) can be equivalent to a homogeneous oblate spheroid of nonlinear conductivity  $\tilde{\sigma}_1$  (see Fig. 5) according to the Maxwell-Garnett formula developed by including  $g_{\perp}$  (Ref. 10)

$$\frac{\tilde{\sigma}_1 - \tilde{\sigma}_s}{\tilde{\sigma}_s + g_{\perp}(\tilde{\sigma}_1 - \tilde{\sigma}_s)} = \rho \frac{\sigma_c - \tilde{\sigma}_s}{\tilde{\sigma}_s + g_{\perp}(\sigma_c - \tilde{\sigma}_s)}, \quad (3)$$

where  $\rho$  is the volume ratio of the core to the whole oblate spheroid. It is worth noting that  $\tilde{\sigma}_1$  herein is the equivalent

nonlinear conductivity along the nonsymmetrical axis of the spheroid whose depolarization factor is  $g_{\perp}$ . [For the symmetrical axis with  $g_{\parallel}$ , the corresponding equivalent nonlinear conductivity can be conveniently achieved by replacing  $g_{\perp}$  with  $g_{\parallel}$  in Eq. (3).] Based on Eqs. (1)–(3), we find that the  $\tilde{\sigma}_1$  is a function of the parameters,  $\sigma_c$ ,  $\sigma_s$ ,  $g_{\perp}$ ,  $\rho$ ,  $\xi_s$ ,  $\chi_s$ , and  $E_s$ . This shows that the nonlinear characteristic in the shell will naturally cause the whole spheroid oblate to possess nonlinear responses in the presence of an external electric field. So far, we might simply reexpress the  $\tilde{\sigma}_1$  of the equivalently homogeneous oblate spheroid as the following nonlinear relation”

$$\tilde{\sigma}_1 = \sigma_1 + \xi_1 \tilde{E}_1 + \chi_1 \tilde{E}_1^2, \quad (4)$$

where  $\sigma_1$  denotes the equivalent linear (field-independent) conductivity,  $\tilde{E}_1$  the equivalent local electric field [Eqs. (7) and (8)], and  $\xi_1$  ( $\chi_1$ ) the equivalent second- (third) order nonlinear susceptibility. Qualitatively, increasing nonlinear responses  $\xi_s$  and  $\chi_s$  of the shell will enhance the equivalent nonlinear responses of the whole oblate spheroid accordingly, i.e., lead to the increase of  $\xi_1$  and  $\chi_1$  of the oblate spheroid in Eq. (4). In this work, for convenience, both  $\xi_1$  and  $\chi_1$  are seen as field-independent real constants, in order to focus on the behavior of harmonic generation (Sec. III B). (In real situations, both of them can vary with the external electric field due to the dependence on  $E_s$ .)

#### B. Harmonic generation in erythrocyte suspensions

Let us start by defining the volume-average electric current density  $\langle \tilde{J} \rangle$  as

$$\langle \tilde{J} \rangle = \tilde{\sigma}_e \tilde{E}_0, \quad (5)$$

where the applied electric field  $\tilde{E}_0 = \tilde{U}/d = E_0 \cos(\omega t)$ . Here  $d$  means the separation between the two circular planes used in the experiments (Fig. 1), and  $\tilde{U}$  the voltage of the suspension which can be measured in our experiment directly. In Eq. (5),  $\tilde{\sigma}_e$  stands for the effective conductivity of the erythrocyte suspension, in which all the symmetrical axis of the erythrocytes are seen to be directed perpendicular to the applied field (due to electro-orientation at the low frequencies of our interest) and their centers are randomly distributed because the erythrocyte along the symmetrical axis is less polarizable in the presence of an electric field with low frequencies. One has also theoretically investigated effective conductivities of a suspension of permeabilized cells by using the finite elements method and the equivalence principle.<sup>24</sup> In view of the known symmetrical Bruggeman effective medium theory,<sup>25,26</sup> we may express the effective conductivity  $\tilde{\sigma}_e$  as the following form (which is developed by adding  $g_{\perp}$ ):

$$p \frac{\tilde{\sigma}_1 - \tilde{\sigma}_e}{g_{\perp} \tilde{\sigma}_1 + (1 - g_{\perp}) \tilde{\sigma}_e} + (1 - p) \frac{\sigma_2 - \tilde{\sigma}_e}{g_{\perp} \sigma_2 + (1 - g_{\perp}) \tilde{\sigma}_e} = 0, \quad (6)$$

where  $p$  is the volume fraction of the erythrocytes. Here  $\sigma_2$  denotes the conductivity of the host liquid, which is assumed to be real and frequency independent. The nonlinear complex conductivity  $\tilde{\sigma}_1$  of the erythrocytes possess the form as

shown in Eq. (4), where  $\sigma_1$  is expressed as a Debye expression,  $\sigma_1 = \sigma_{1H} + \delta\sigma / (1 + if/f_0)$ . Here  $\sigma_{1H}$  is the conductivity at high frequency,  $\delta\sigma$  the dispersion strength of the erythrocytes,  $f_0$  the intrinsic characteristic frequency,  $f$  the frequency of the external field, and  $i = \sqrt{-1}$ . More discussion on Eq. (4) can be found in Sec. V. In Eq. (4), we adopt  $\tilde{E}_1 \approx \langle \tilde{E}_1 \rangle$ , and there exists

$$\langle \tilde{E}_1 \rangle = \frac{\tilde{\sigma}_e}{\tilde{\sigma}_e + g_\perp(\tilde{\sigma}_1 - \tilde{\sigma}_e)} \tilde{E}_0, \quad (7)$$

which is obtained by solving the Maxwell equations. Here  $\langle \dots \rangle$  denotes the volume average of  $\dots$ . For convenience, we also adopt  $\tilde{E}_1^2 \approx \langle \tilde{E}_1^2 \rangle$ . Here  $\langle \tilde{E}_1^2 \rangle$  is determined by<sup>25,27</sup>

$$\langle \tilde{E}_1^2 \rangle = \frac{\tilde{E}_0^2}{p} \frac{\partial \tilde{\sigma}_e}{\partial \tilde{\sigma}_1}. \quad (8)$$

Next, the electric current density  $\langle \tilde{J} \rangle$  [Eq. (5)] can be expressed in the form of harmonics

$$\langle \tilde{J} \rangle = J_{dc} + J_\omega \cos(\omega t) + J_{2\omega} \cos(2\omega t) + J_{3\omega} \cos(3\omega t), \quad (9)$$

where  $J_{dc}$ ,  $J_\omega$ ,  $J_{2\omega}$ , and  $J_{3\omega}$  stand for the dc component, basic harmonics, second harmonics, and third harmonics of the current density, respectively. Such harmonics can be numerically extracted by using the orthogonal theorem of the trigonometric functions like  $\cos(\omega t)$ ,  $\cos(2\omega t)$ , and  $\cos(3\omega t)$ . In Eq. (9), higher-order harmonics, e.g.,  $J_{4\omega}$  and  $J_{5\omega}$ , have been neglected because their strengths are much smaller.

As in experiments only the real part of the current density  $\langle \tilde{J} \rangle$  can be measured, the ratio of current harmonics,  $I_{3\omega}/I_\omega$ , obtained from our experiments, are identical to the ratio of current-density harmonics,  $\text{Re}(J_{3\omega})/\text{Re}(J_\omega)$ , due to the relation between  $\text{Re}(\langle \tilde{J} \rangle)$  and  $\tilde{I}$ , i.e.,  $\tilde{I} = \text{Re}(\langle \tilde{J} \rangle)S$ . Here,  $\text{Re}(\dots)$  means the real part of  $\dots$ , and  $S$  the area of the electric circular plane used in the experiments. For the comparison between our experimental observations and theoretical analysis, there exist

$$\frac{I_{2\omega}}{I_\omega} = \frac{\text{Re}(J_{2\omega})}{\text{Re}(J_\omega)}, \quad (10)$$

$$\frac{I_{3\omega}}{I_\omega} = \frac{\text{Re}(J_{3\omega})}{\text{Re}(J_\omega)}. \quad (11)$$

#### IV. RESULTS

Now we are allowed to use Eqs. (10) and (11) to interpret the experimental data displayed in Figs. 2–4. To comply with our experiment, only the voltage used in the experiment is adopted for the theoretical fitting displayed by Figs. 2–4, namely,  $\tilde{U} = 5.0$  V (Fig. 2),  $\tilde{U} = 6.6$  V (Fig. 3), and  $\tilde{U} = 8.3$  V (Fig. 4), whereas all the other parameters are kept unchanged, see the caption of Fig. 2 for details. Apparently, excellent agreement between the theory and experiment is shown. When the matter consisting of conductive particles having nonlinear characteristics [Eq. (4)] is subjected to an ac field, the electric response will consist of ac fields at fre-

quencies of the higher-order harmonics (harmonic generation) [Eq. (9)]. Thus, we can safely conclude that the harmonics come from nonlinear characteristics of conductivities of erythrocytes (such characteristics are due to ion translocation). In detail, as the frequency of the external electric field increases, both second- and third-harmonic currents are caused to decrease. In other words, lower frequency yields stronger harmonic responses. This is because lower frequencies can yield more sufficient field amplification for the nonlinear responses. On the other hand, as the frequency is higher, the protein conformational change becomes smaller, which yields less ion translocation and thus smaller strength of harmonics. If the voltage of the emf is increased, the harmonic responses are shown to be enhanced increasingly due to the more amplified net field modulation across the plasma membrane of the erythrocytes. Finally, we should mention that, as potassium continues to leave the cell, separating more charges, the membrane potential (or alternatively, transmembrane voltage) will continue to grow. Though the frequency behavior of the induced transmembrane potential depends on the external conductivity, it exhibits a plateau-like behavior at low frequencies.<sup>28</sup>

We should remark that odd harmonics can appear for both asymmetrical and symmetrical structures, but even harmonics can only appear for asymmetrical structures. The second-harmonic generation of our interest is related to a certain internal asymmetry of the electric characteristics of the erythrocyte, which we believe arises from the membrane protein conformational changes. In this work, we have investigated second and third harmonics only. As a matter of fact, higher-order (e.g., fourth or fifth) harmonics of currents also exist. However, their magnitudes are much smaller.

As the lowest-order even harmonic generation, the second-harmonic generation (SHG) owns the strongest strength among all even harmonic generations. The lower analysis on the origin of second-harmonic generation also holds for higher-order even harmonic generation. Materials lacking inversion symmetry can exhibit a so-called second-order nonlinearity.<sup>29</sup> This can give rise to the phenomenon of SHG, i.e., an input (pump) field can generate another field with twice the frequency in the medium, namely, the second-harmonic field. The physical mechanism behind SHG can be understood as follows. Due to the second-order nonlinearity, the fundamental (pump) field generates a nonlinear polarization which oscillates with twice the fundamental frequency. According to Maxwell's equations, this nonlinear polarization induces a field with this doubled frequency. The SHG effect, like the third-order Kerr-type coefficient, involves the nonlinear susceptibilities of the constituents and local field enhancement which arises from the structure of composite materials. For example, Hui *et al.* studied a dilute suspension of coated particles with the shell having a nonlinear susceptibility for SHG,<sup>30</sup> and one of us designed a class of ferrofluid-based soft nonlinear optical materials with enhanced SHG with magnetic-field controllabilities.<sup>31</sup>

Theoretical<sup>32</sup> and experimental<sup>33,34</sup> reports also suggested that spherical particles exhibit a rather unexpected and nontrivial SHG due to the broken inversion symmetry at particle surfaces, despite their central symmetry which seem-



ingly prohibits second-order nonlinear effects. In colloidal suspensions, the SHG response for centrosymmetric particles was experimentally reported.<sup>33,34</sup> Most recently, SHG was also shown to appear for spherical semiconductor nanocrystals.<sup>35</sup> So far, the SHG from centrosymmetrical structure has received an extensive attention.<sup>32–34,36,37</sup> Thus, for the erythrocytes assumed to exist in the shape of oblate spheroid in this work, we have used Eq. (4)

$$\tilde{\sigma}_1 = \sigma_1 + \xi_1 \tilde{E}_1 + \chi_1 \tilde{E}_1^2,$$

where the term  $\xi_1 \tilde{E}_1$  comes from the second-order nonlinearity. Throughout the paper, the external applied field used in both theory and experiment is only ac fields,  $\tilde{E}_0 = E_0 \cos(\omega t)$ . According to Eq. (4), both even and odd harmonics can be caused to appear, as already shown in Eq. (9). On the other hand, if the term  $\xi_1 \tilde{E}_1$  (second-order nonlinearity) disappears due to the perfect symmetry of the erythrocytes, namely,

$$\tilde{\sigma}_1 = \sigma_1 + \chi_1 \tilde{E}_1^2, \quad (12)$$

only odd harmonics will then be induced due to the ac fields,  $\tilde{E}_0 = E_0 \cos(\omega t)$ :

$$\langle \tilde{J} \rangle = J_\omega \cos(\omega t) + J_{3\omega} \cos(3\omega t). \quad (13)$$

However, for Eq. (12), if both ac and dc electric fields are applied,  $\tilde{E}_0 = E_{dc} + E_{ac} \cos(\omega t)$ , both even and odd harmonics will appear again:

$$\langle \tilde{J} \rangle = J_{dc} + J_\omega \cos(\omega t) + J_{2\omega} \cos(2\omega t) + J_{3\omega} \cos(3\omega t). \quad (14)$$

It is worth noting that the harmonics expressed in Eq. (14) have the different physical origin from those expressed in Eq. (9), even though both Eqs. (9) and (14) have the same mathematical form. In addition, the higher-order harmonics in both Eqs. (13) and (14) have been omitted because they are often much smaller than the lower-order ones.

Finally, for all the equations, Eqs. (9), (13), and (14), we have mentioned that the higher-order harmonics (e.g., fourth, fifth, sixth, and so on) in them have been omitted because they are often much smaller than the lower-order ones, even though Eqs. (4) and (12) have been used where the highest-order nonlinearity is third-order only. This has implied the fact that low-order nonlinearity can induce high-order harmonic generations. For some more details, we refer the reader to Ref. 38 (Appendix A).

## V. DISCUSSION AND CONCLUSION

Here some comments are in order. Our experimental data were measured for living cells suspensions. We have also conducted experiments on dead cells. It is found that dead cells have almost no harmonic responses. This shows that our method can be used to distinguish living and dead cells. Owing to the aforementioned geometrical effects, the present method can also be used to distinguish different shapes of the same sort of cells. In this sense, our results are expected to be of some biophysical relevance.

The present experiments were conducted in the frequency range from some hertz up to 3 kHz. In this range, electrode polarization probably plays a role.<sup>39–42</sup> In our experimental setup, the electrode is made of pure copper. To test the possible electrode effects, we have, respectively, measured the saccharose solution and dead erythrocytes in the same setup as the living erythrocytes, and found that there are almost no harmonic responses within the range of the voltage and frequency of our interest. This shows that the electrode polarization (and the host saccharose solution) does not play an evident role in our measurement of the nonlinear effects. Owing to the exclusion of the contributions of both electrode polarization and the host saccharose solution, the nonlinearities should be caused to appear by the ion translocation due to the simple structure (i.e., lipid encapsulated hemoglobin) of erythrocytes, as expected.

In our experiment, by intense sucrose washing, we were intended to free the samples from the ions of other ingredients in the blood, e.g., leukocytes. After this treatment, the cells in our measurement were driven into the Donnan equilibrium, namely, the distribution of ion species between two ionic solutions separated by a membrane.<sup>43</sup>

To sum up, we have investigated nonlinear ac responses of erythrocytes, and found that both even and odd harmonics are sensitive to cell shapes, conductivities, field frequencies, and field magnitude. Good agreement between theory and experiment has been shown. It becomes possible to detect nonlinear characteristics, shapes and conductivities of erythrocytes by measuring such ac responses.

## ACKNOWLEDGMENTS

This work was supported by the National Natural Science Foundation of China under Grant Nos. 1024402, 10574027, and 10604014, by the “973” project of Ministry of Science and Technology of China (2005CB523306), by the Shanghai Science and Technology Committee (05DZ19747), by the Shanghai Education Committee and the Shanghai Education Development Foundation (“Shu Guang” project), by the Pujiang Talent Project (No. 06PJ14006) of the Shanghai Science and Technology Committee, and by Chinese National Key Basic Research Special Fund under Grant No. 2006CB921706.

<sup>1</sup>B. L. McClain, I. J. Finkelstein, and M. D. Fayer, *J. Am. Chem. Soc.* **126**, 15702 (2004).

<sup>2</sup>L. Haider, P. Snabre, and M. Boynard, *Biophys. J.* **87**, 2322 (2004).

<sup>3</sup>D. R. Daniels, J. C. Wang, R. W. Briehl, and M. S. Turner, *J. Chem. Phys.* **124**, 024903 (2006).

<sup>4</sup>G. M. Grotenbreg *et al.*, *J. Am. Chem. Soc.* **128**, 7559 (2006).

<sup>5</sup>E. J. Ding and C. K. Aidun, *Phys. Rev. Lett.* **96**, 204502 (2006).

<sup>6</sup>S. Kaufmann and M. Tanaka, *ChemPhysChem* **4**, 699 (2003).

<sup>7</sup>S. B. Rochal and V. L. Lorman, *Phys. Rev. Lett.* **96**, 248102 (2006).

<sup>8</sup>L. C. L. Lin, N. Gov, and F. L. H. Brown, *J. Chem. Phys.* **124**, 074903 (2006).

<sup>9</sup>R. D. Schaller, J. C. Johnson, and R. J. Saykally, *ChemPhysChem* **4**, 1243 (2003).

<sup>10</sup>J. P. Huang and K. W. Yu, *J. Chem. Phys.* **121**, 7526 (2004).

<sup>11</sup>L. Gao, L. P. Gu, and Z. Y. Li, *Phys. Rev. E* **68**, 066601 (2003).

<sup>12</sup>T. B. Jones, *Electromechanics of Particles* (Cambridge University Press, New York, 1995).

<sup>13</sup>A. M. Woodward, A. Jones, and X. Zhang, *Bioelectrochem. Bioenerg.* **40**, 99 (1996).

<sup>14</sup>N. Gov, *Phys. Rev. Lett.* **93**, 268104 (2004).

- <sup>15</sup>R. D. Astumian, Phys. Rev. Lett. **91**, 118102 (2003).
- <sup>16</sup>D. Nawarathna, J. H. Miller, Jr., J. R. Claycomb, G. Cardenas, and D. Warmflash, Phys. Rev. Lett. **95**, 158103 (2005).
- <sup>17</sup>T. Y. Tsong and R. D. Astumian, Bioelectrochem. Bioenerg. **15**, 457 (1986).
- <sup>18</sup>R. D. Astumian and I. Derényi, Eur. Biophys. J. **27**, 474 (1998).
- <sup>19</sup>B. Chanda, O. K. Asamoah, R. Blunck, B. Roux, and F. Bezanilla, Nature (London) **436**, 852 (2005).
- <sup>20</sup>C. L. Davey, H. M. Davey, and D. B. Kell, Bioelectrochem. Bioenerg. **28**, 319 (1992).
- <sup>21</sup>A. M. Woodward and D. B. Kell, Bioelectrochem. Bioenerg. **24**, 83 (1990).
- <sup>22</sup>L. D. Landau, E. M. Lifshitz, and L. P. Pitaevskii, *Electrodynamics of Continuous Media*, 2nd ed. (Pergamon, New York, 1984), Chap. II.
- <sup>23</sup>J. Gimsa and D. Wachner, Biophys. J. **77**, 1316 (1999).
- <sup>24</sup>M. Pavlin and D. Miklavčič, Biophys. J. **85**, 719 (2003).
- <sup>25</sup>J. P. Huang and K. W. Yu, Phys. Rep. **431**, 87 (2006).
- <sup>26</sup>D. A. G. Bruggeman, Ann. Phys. (Leipzig) **24**, 636 (1935).
- <sup>27</sup>D. Stroud and P. M. Hui, Phys. Rev. B **37**, 8719 (1988).
- <sup>28</sup>J. Gimsa and D. Wachner, Biophys. J. **81**, 1888 (2001).
- <sup>29</sup>Y. R. Shen, *The Principles of Nonlinear Optics* (Wiley, New York, 1984).
- <sup>30</sup>P. M. Hui and D. Stroud, J. Appl. Phys. **82**, 4740 (1997).
- <sup>31</sup>C. Z. Fan and J. P. Huang, Appl. Phys. Lett. **89**, 141906 (2006).
- <sup>32</sup>J. I. Dadap, J. Shan, K. B. Eisenthal, and T. F. Heinz, Phys. Rev. Lett. **83**, 4045 (1999).
- <sup>33</sup>N. Yang, W. E. Angerer, and A. G. Yodh, Phys. Rev. Lett. **87**, 103902 (2001).
- <sup>34</sup>S. H. Jen and H. L. Dai, J. Phys. Chem. B **110**, 23000 (2006).
- <sup>35</sup>D. H. Son, J. S. Wittenberg, U. Banin, and A. P. Alivisatos, J. Phys. Chem. B **110**, 19884 (2006).
- <sup>36</sup>P. Xu, S. H. Ji, S. N. Zhu, X. Q. Yu, J. Sun, H. T. Wang, J. L. He, Y. Y. Zhu, and N. B. Ming, Phys. Rev. Lett. **93**, 133904 (2004).
- <sup>37</sup>R. Bernal and J. A. Maytorena, Phys. Rev. B **70**, 125420 (2004).
- <sup>38</sup>W. J. Tian, J. P. Huang, and K. W. Yu, Phys. Rev. E **73**, 031408 (2006).
- <sup>39</sup>H. P. Schwan, in *Physical Techniques in Biological Research*, edited by W. L. Nastuk (Academic, New York, 1963), pp. 323–407.
- <sup>40</sup>H. P. Schwan, Ann. N. Y. Acad. Sci. **148**, 191 (1968).
- <sup>41</sup>H. P. Schwan and B. Onaral, Med. Biol. Eng. Comput. **23**, 28 (1985).
- <sup>42</sup>K. R. Foster and H. P. Schwan, in *Handbook of Biological Effects of Electromagnetic Radiation*, 2nd ed., edited by C. Polk and E. Postow (CRC Press, Boca Raton, FL, 1997), pp. 25–102.
- <sup>43</sup>J. Gimsa, T. Schnelle, G. Zechel, and R. Glaser, Biophys. J. **66**, 1244 (1994).